2008

Development Of Method For Measurement Of Passive Losses In Cr2+:Znse And Cr2+:Zns Laser Crystals Using Polarized Laser Beam

Anitha Arumugam
University of Alabama at Birmingham

DEVELOPMENT OF METHOD FOR MEASUREMENT OF PASSIVE LOSSES IN CR^{2+}:ZNSE AND CR^{2+}:ZNS LASER CRYSTALS USING POLARIZED LASER BEAM

by

ANITHA ARUMUGAM

Dr. SERGEY MIROV, COMMITTEE CHAIR
Dr. SERGEY VYAZOVKIN
Dr. VLADIMIR FEDOROV

A THESIS

Submitted to the graduate faculty of The University of Alabama at Birmingham,
in partial fulfillment of the requirements for the degree of
Master of Science

BIRMINGHAM, ALABAMA

2008

DEVELOPMENT OF METHOD FOR MEASUREMENT OF PASSIVE LOSSES IN CR^{2+}:ZNSE AND CR^{2+}:ZNS LASER CRYSTALS USING POLARIZED LASER BEAM

ANITHA ARUMUGAM

PHYSICS

ABSTRACT

Measurement of total attenuation in transition metal doped crystals is still an opened field and needs further research and development. In this investigation we developed a method for measurement of passive losses in Cr^{2+}:ZnSe and Cr^{2+}:ZnS laser crystals using polarized laser beam. A method for loss measurement, the Transmission Comparison Method, has been taken into consideration and modified to quantify the sample loss which in our case is larger than the extremely small loss measured in the Transmission Comparison Method. The developed method was then used to measure the surface reflectivity losses, intrinsic material absorption, and internal volumetric scattering, all of which were initially lumped together as total transmission losses.

The experimental setup was assembled and validated by measuring the front surface reflection transmission and comparing with the theoretical data. Two undoped ZnSe polycrystalline samples with different lengths were used in the measurements. The effective absorption coefficient calculated from the measured data and the internal absorption coefficient extracted from the spectrophotometer measurements were used to estimate the internal scattered coefficient. The internal scattered coefficient was calculated to be $0.019cm^{-1}$ for both laser crystals.

ACKNOWLEDGEMENTS

I thank my advisor Dr.Sergey Mirov for supporting, guiding and helping me in my research work. I am grateful to him for all the support extended to me in many ways during the past three years, and will always value him as an excellent teacher.

I thank Professors Dr.Sergey Vyazovskin and Dr.Vladimir Fedorov for being my graduate committee members and providing valuable feedback on my research.

I thank Dr.Yogesh Vohra for his guidance and encouragement during my graduate studies.

Special thanks to Dr. Igor Moskalev for guiding, helping, and extending technical advices on completing the research and thesis.

Also I appreciate all the support from faculty members and staffs of the Department of Physics and the help and friendship of fellow graduate students.

Here I specially express my deepest thanks to my husband and my parents for the encouragement and support during my graduate studies.

TABLE OF CONTENTS

Page

LIST OF TABLES

Table *Page*

LIST OF FIGURES

Figure *Page*

CHAPTER 1

INTRODUCTION

1.1 Motivation

Broadly tunable middle-infrared (mid-IR) lasers are desirable for many scientific, medical, sensing, and military applications. Transition metal (TM^{2+}, e.g., Cr^{2+} or Fe^{2+}) doped chalcogenide crystals represent a unique class of solid state gain media with strong and ultra-broad absorption and emission bands promising for mid-IR lasing at room temperature (RT). In 1996, scientists from the Lawrence Livermore National Laboratory [1] were first to demonstrate that among different types of crystalline gain materials, TM^{2+} doped wide bandgap II-VI semiconductor crystals are very special for mid-IR lasing. These wide bandgap TM^{2+} doped II-VI compounds have several important features that distinguish them from other oxide and fluoride laser crystals. These features are as follows: (i) the heavy anions in the crystals provide a very low energy optical phonon cutoff that, on one hand, makes them transparent in a wide spectral region and, on the other, decreases the efficiency of non-radiative decay, enabling a high yield of fluorescence at RT; (ii) II-VI compounds tend to crystallize as tetrahedrally coordinated structures at the dopant site. Tetrahedral coordination gives smaller crystal field splitting compared to the typical octahedral coordination, placing the dopant transitions further into the IR. Active interest in TM doped II-VI compounds is explained by the fact that, in addition to attractiveness for effective mid-IR RT lasing, these media are close mid-IR analogs of the titanium-doped sapphire (Ti-S) in terms of spectroscopic and laser characteristics and it was anticipated that TM^{2+} doped chalcogenides will lase in the mid-IR with a great variety of possible regimes of oscillation, similar to the Ti-S laser. Indeed,

recently, Cr^{2+} doped chalcogenide (mainly ZnSe, ZnS, and CdSe) lasers have emerged as an attractive source of tunable laser radiation in the 2-3.6μm region (see review [1] and references herein).

Currently the state of the art in TM:II-VI laser systems rely either on a single crystal, or polycrystalline vapor grown materials. Both of these materials have particular drawbacks in terms of crystal doping. The commonly used doping methods are in melt [2], vapor growth [3,4], and after growth thermo-diffusion doping [5]. Under atmospheric pressure ZnSe sublimation occurs at a temperature above ~400 °C which is lower than that of the melting point [2]. Therefore to use the melt growth techniques, in addition to high temperature (1515 °C), it is necessary to apply high pressure ($75x10^2$ KPa) [2]. High temperature melt growth is often accompanied by uncontrolled contamination which can lead to undesirable and parasitic absorptions. Control of the amount of Cr^{2+} ions incorporated in the crystal is difficult when using the vapor growth techniques [3,4]. Host crystals/polycrystals that are already grown allow for another method of TM incorporation, the thermal diffusion doping. Currently most widely used for fabrication of Cr-doped chalcogenide laser crystals this technique utilizes thermally activated diffusion of transition metal ions into the polycrystalline II-IV crystals [6]. However, polycrystalline chalcogenides' post-growth thermal diffusion can be accompanied by the grain size growth and associated scattering and absorption losses.

For effective mid-IR lasing chromium doped gain materials with low losses are needed. The lack of understanding of the nature of losses in the chromium doped crystals prepared by post growth thermal diffusion motivated the proposed research. It is proposed to use an optical technique to differentiate between internal volumetric scattering, intrinsic

absorption, and surface reflection losses in the laser crystals, and to identify major factors defining passive losses in Cr doped chalcogenides (Cr concentration, temperature, and exposition time of annealing) for future optimization of these parameters.

Determination of the total attenuation represents a difficult problem. For measuring the total attenuation in the polycrystalline materials, few methods are known such as: (A) transmission comparison method; (B) calorimetric method; (C) two-beam method by Tynes.

With the (A) transmission comparison method [6,7], transmission of samples of different lengths is compared. The attenuation is then calculated from the difference in transmission of the samples of different lengths. Through this method, extremely small sample losses are measurable but the drawback of this method is that for highly accurate measurements, large number of precision polished samples with the same surface quality is required.

In the (B) calorimetric method [8,9] case, the rise of sample temperature is measured when an intense light beam passes through the crystal. Then the attenuation is calculated from the rate of the temperature rise. This method probably yields highly accurate values. But, the drawback of this method is that it requires highly sensitive equipment for precision measurement of the sample temperature rise and difficulty in differentiation between scattering and internal absorption.

(C) Tynes two-beam method [10,11,12] starts from a laser beam that is split into a sample and a reference beam. The sample beam is linearly polarized, passes through sample at the Brewster angle and strikes the first detector. The reference beam is measured at the second detector. The photocurrents at both detectors are compared, where the

produced ac signal corresponds to the sum of surface losses and attenuation in the sample. Although this method requires a single sample, it is difficult to differentiate between the surface and volume loss through this method.

This summary shows that measurement of attenuation in transition metal doped crystals is still an opened field and needs further research and development. So, a loss measurement method which requires single sample has to be developed and through this method we should be able to discriminate between the internal losses.

In the development of our method, method (A) has been taken into consideration and modified as follows: Originally, method (A) was used for measurements of extremely small internal losses in high-quality optical glasses used for fabrication of long (kilometers) optical fibers. In that case, the extremely small internal volumetric losses in practically usable high-quality optical glass samples are comparable to the surface loss (due to non-ideal polishing or surface contamination). However, in the case of polycrystalline II-VI materials, the internal scattering is usually much higher than that in optical glasses. As a result, the surface losses of well polished II-VI polycrystalline samples (such as ZnSe and ZnS) are much smaller than the internal scattering losses and can be safely ignored. This allows us to simplify the (A) method by excluding precision measurements of the surface loss.

Another important modification of the method (A) is that instead of spectrally broadband lamp light source here we use a polarized, narrow-linewidth laser beam. The advantages of laser beam measurements include: higher spatial resolution, higher signal to noise (S/N) ratio, and high spectral selectivity.

The use of monochromatic and spatially narrow laser beam allows for another important improvement of the method: instead of many samples of different lengths here we use a single thick and long sample which is rotated in the plane of incidence of the laser beam. Due to refraction of the beam in the sample the propagation path of the beam through the material is changed as the sample is rotated. As a result, we can obtain virtually unlimited set of measurements of transmission at many different lengths using only one sample. In practice, however, we used two such samples of different thicknesses to further improve the accuracy of our measurements.

1.2 Research Goals

The overall goals of this investigation are:

- To develop a method for measurement of passive losses in Cr^{2+}:ZnSe and Cr^{2+}:ZnS laser crystals using polarized laser beam.
- To measure the passive losses in Cr^{2+}:ZnSe and Cr^{2+}:ZnS laser crystals with high accuracy using polarized laser beam.
- To discriminate between scattering, reflectivity and absorption components, all lumped together as total transmission losses, in the polarized light transmission measurements.
- To monitor the total optical loss caused by internal scattering and absorption of the initially undoped polycrystalline ZnSe and ZnS host materials.

1.3 Research Aims

Aim 1: Assemble the experimental set-up for measurement.

Aim 2: Validate the performance of experimental set-up by measuring the volumetric losses in initially undoped ZnSe polycrystalline samples and its comparing with the theoretical data.

Aim 3: Measure the passive losses in initially undoped ZnSe laser crystals with the assembled experimental setup and discriminate between scattering, reflectivity and absorption components.

CHAPTER 2

EXPERIMENTAL WORK

2.1 Basic Consideration of the Polarized Laser Beam Method

In our experiment, we considered using the transmission comparison method of polarized beam to separately measure scattering, reflection, and intrinsic losses in initially undoped polycrystalline ZnSe host materials. It is based on simultaneous measurement of transmission of the polarized laser beam through the laser crystal and reflected and scattered light from both facets of the laser crystal. This approach will allow for accurate extraction of intrinsic volumetric loss in the laser crystal. The initially proposed schematic diagram of the method is depicted in Figure 2.1.

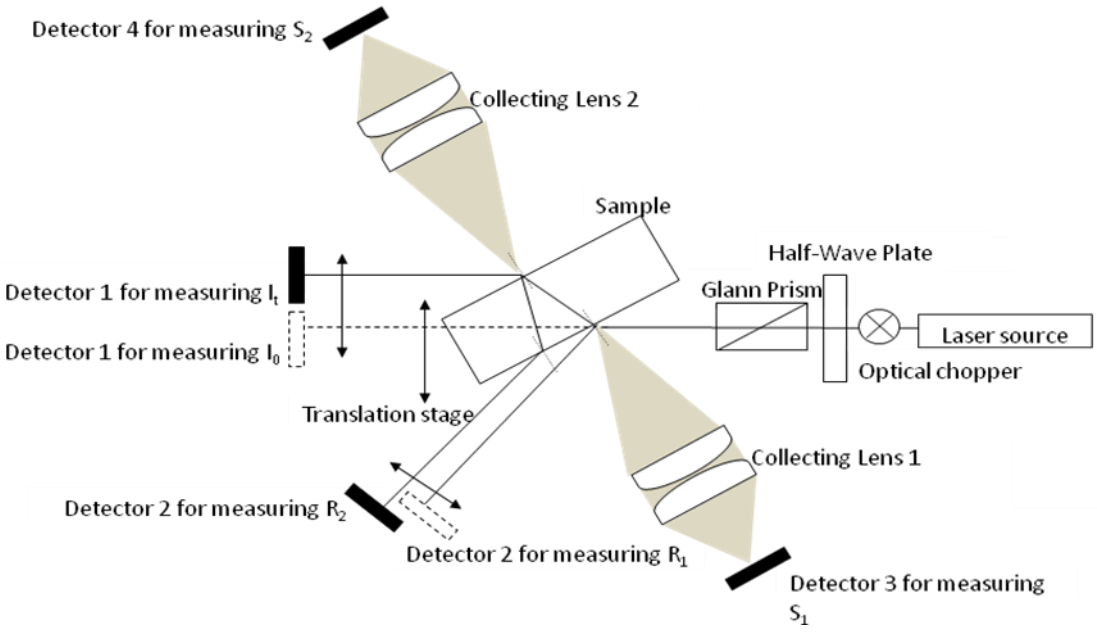

Figure 2.1. Initially proposed experimental set-up for measuring scattering, reflection, and intrinsic losses.

As proposed for convenience of light detection and improving signal to noise ratio, the incident beam from laser source is chopped by using optical chopper (see Fig.2.1). To avoid saturation of detectors the beam is further attenuated by a combination of half-wave plate and Glann prism. Measurement will begin from measuring the polarized pulsed incident beam intensity, I_0 at detector 1 without the laser crystal placed in the beam path (shown by dashed line in Fig.2.1). After this measurement the laser crystal will be introduced in the beam path and detector 1 will be repositioned to measure the transmitted beam intensity, I_t. The reflected beams intensity will be measured by using detector 2. The front surface and back surface of the laser crystal scattered lights will be collected by the collecting lens into the detector 3 and 4, respectively.

During the experimental set-up it was noticed that the scattered beam intensity ratio to the transmitted and reflected beam intensity was extremely small. So, the laser crystal front and back surface scattered light intensity is considered negligible and decided not to be measured. The new schematic diagram of the experimental set-up for the measurement method is shown in Figure 2.2. He-Ne laser beam with wavelength 632.8nm is aligned to be at the height of 17.5cm from the optical table by using prism 1 and prism 2. The reason for choosing beam wavelength, 632.8 nm can be explained using Figure 2.3. As depicted in the figure, a strong Cr^{2+} absorption is observed over 1400 - 2300nm spectral range. To eliminate active sample absorption in the measurements, the incident beam wavelength over this range has to be avoided. To avoid strong charge transfer absorption associated with $Cr^{2+} + e_v \rightarrow Cr^{+}$ transition in ZnS and ZnSe crystal the laser wavelength should be longer than 630nm.

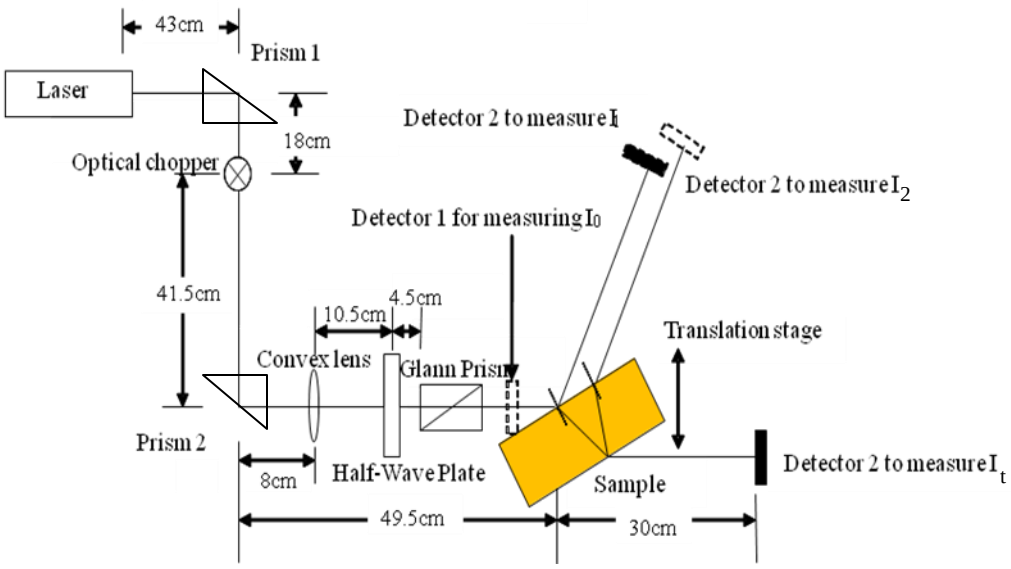

Figure 2.2. Final Experimental set-up for measuring scattering, reflection, and intrinsic losses.

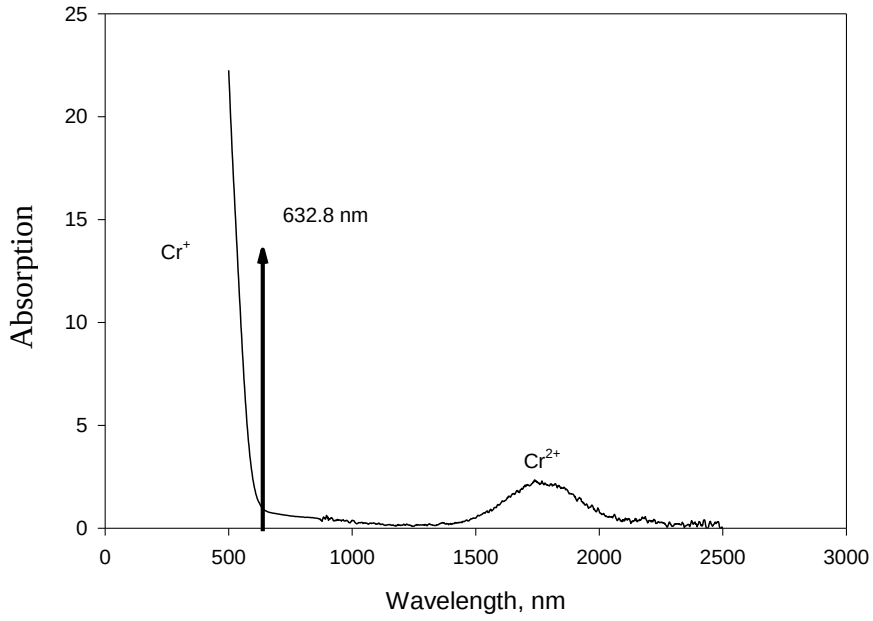

Figure 2.3. Absorption spectrum of diffusion doped Cr:ZnSe gain element.

Although, the best choice of excitation wavelengths is in the 1000-1300 nm wavelength range or longer than 2500nm, considering the availability, He-Ne laser with wavelength 632.8 nm is chosen.

The optical chopper is placed in between prism 1 and prism 2. Since the laser beam size was larger than the height of the sample, focusing lens with 20cm focal length has been introduced in front of prism 2 to reduce the beam size. To avoid saturation of detectors the beam intensity is attenuated by a combination of half-wave plate and Glann prism. Mechanical rotational stage, which holds the laser crystal and can be rotated mechanically to a precise angular position, is mounted on a translation stage and placed in front of Glann prism. Then detector 1 is placed in between the Glann Prism and rotational stage and the incident beam intensity, I_0 is measured. After this measurement, detector 1 is removed from the beam path, and the first surface reflected beam intensity I_1 is measured at detector 2. By repositioning detector 2 the other first surface reflected beam intensity I_2 is measured. Again, by repositioning detector 2 the second surface transmitted beam intensity I_t is measured. So, 4 parameters are measured. This measurement will be repeated for few incident angles θ by rotating the mechanical rotator which holds the sample.

Figure 2.4 shows the schematic diagram of the measurement method. A laser beam with intensity I_0 hits the input surface S_1 of the laser crystal at an incident angle θ at the point *A* of the surface. A part of the beam is reflected by the surface and its intensity is denoted as $I_1(\theta)$. Therefore, after the beam passes through the surface, its intensity reduces to $I_A(\theta)$. Then the beam passes through the volume of the laser crystal and propagates a distance $d(\theta)$ until it hits the second surface S_2 at point *B.* Due to

volumetric scattering loss the beam intensity near the second surface, denoted as $I_B(\theta)$, is smaller than the initial beam intensity $I_A(\theta)$. On the second surface of the crystal S_2 a part of the laser beam is transmitted by the surface and its intensity becomes $I_t(\theta)$. Another portion of the beam is reflected by the surface with intensity $I'_B(\theta)$. The reflected beam further propagates through the crystal towards surface S_1 and again passes distance $d(\theta)$ until it hits the surface at point *C*. Due to volumetric scattering loss the beam intensity $I_C(\theta)$ at point *C* (right before it leaves the crystal) is smaller than the initial beam intensity $I'_B(\theta)$. On the surface S_1 a part of the beam is transmitted by the surface and its intensity is denoted as $I_2(\theta)$.

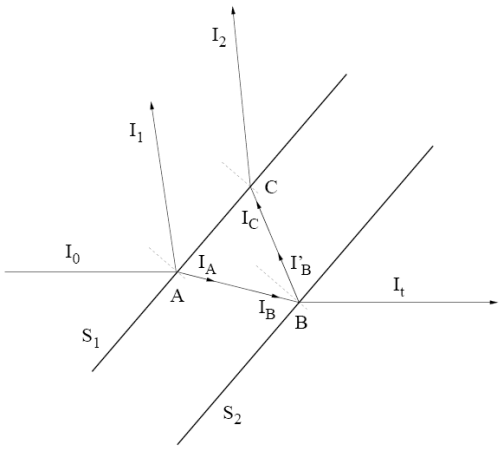

Figure 2.4. Schematic diagram of the "Transmitted - Beam" method. The beam enters the plane parallel crystal from left.

2.2 Calibration of Half-Wave Plate Angle for the Right Intensity

To choose the right intensity of laser beam for measurements, half-wave plate was calibrated at different angles and the beam intensities: I_0, I_t, I_1 and I_2 were measured.

Undoped ZnSe laser crystal has been used throughout this measurement. Measurements began from measuring the polarized pulsed incident beam intensity I_0 at detector 2 (shown in Fig.2.2). Half-wave plate was calibrated from the minimum to maximum intensity detected by the detector. The corresponding angle to the detected beam intensities shown on the half wave plate holder lies from 42° to 84°. Half-wave plate was calibrated from 42° to 84° and the detected beam intensities were recorded. Table 2.1 shows the detected incident beam intensities for corresponding Half-wave plate angles.

Table 2.1: Incident beam power vs half-wave plate angle

Half-wave plate angle (°)	Incident Beam power P_0 (V)
42	0
44	0.125
46	0.500
48	0.875
50	1.375
52	2.250
54	2.875
56	3.875
58	4.750
60	5.875
62	6.875
64	8.000
66	9.000
68	10.000
70	10.750
72	11.750
74	12.500
76	13.500
78	14.000
80	14.500
82	14.750
84	15.000

By plotting graph for the measured angles, the incident beam intensities I_0 for each calibrated half-wave plate angle were obtained. Then, this measurement was repeated by placing the detector about 30 cm in front of the sample and the transmitted beam intensities I_t was measured and recorded. Figure 2.5 shows the plot of transmission I_t / I_0 vs incident beam intensity I_0.

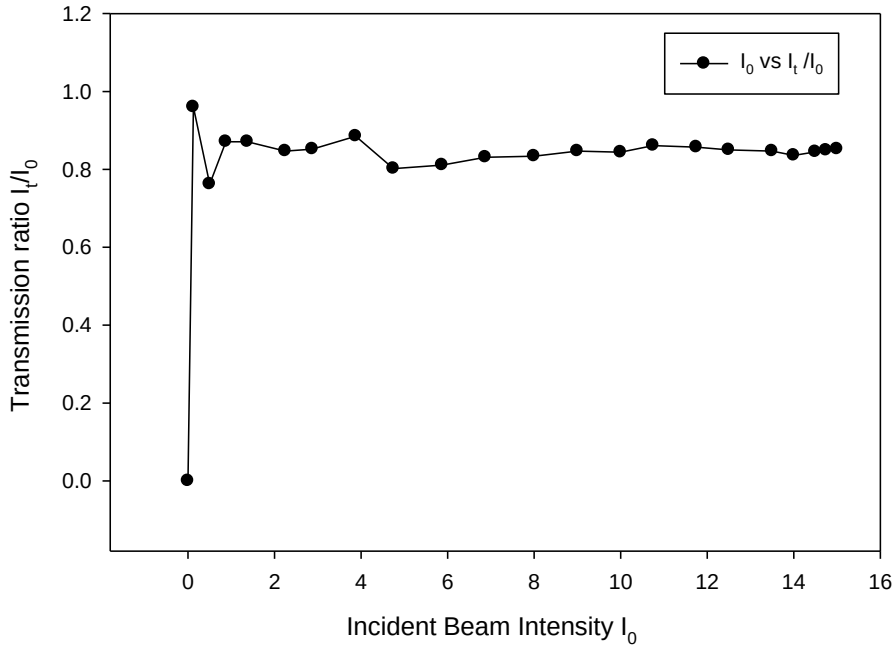

Figure 2.5.Transmission I_t / I_0 vs incident beam intensity I_0

Then the reflected beam intensity I_1 was measured by detector 1 and recorded. Figure 2.6 shows the plot of transmission I_1 / I_0 vs incident beam intensity I_0. Similarly, by repositioning detector 1 the reflected beam intensity I_2 was measured and recorded. Figure 2.7 shows the plot of transmission I_2 / I_0 vs incident beam intensity I_0.

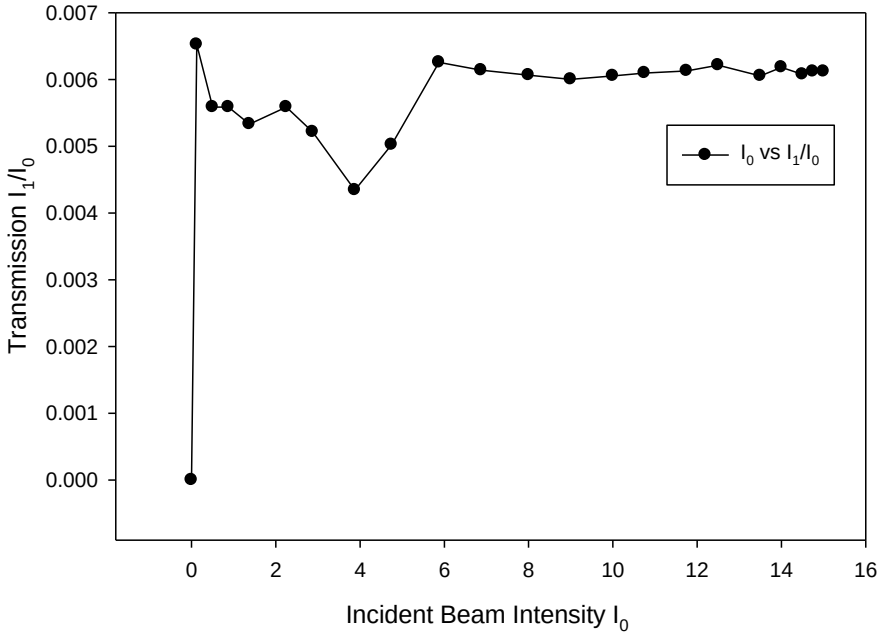

Figure 2.6. Transmission I_1 / I_0 vs incident beam intensity I_0

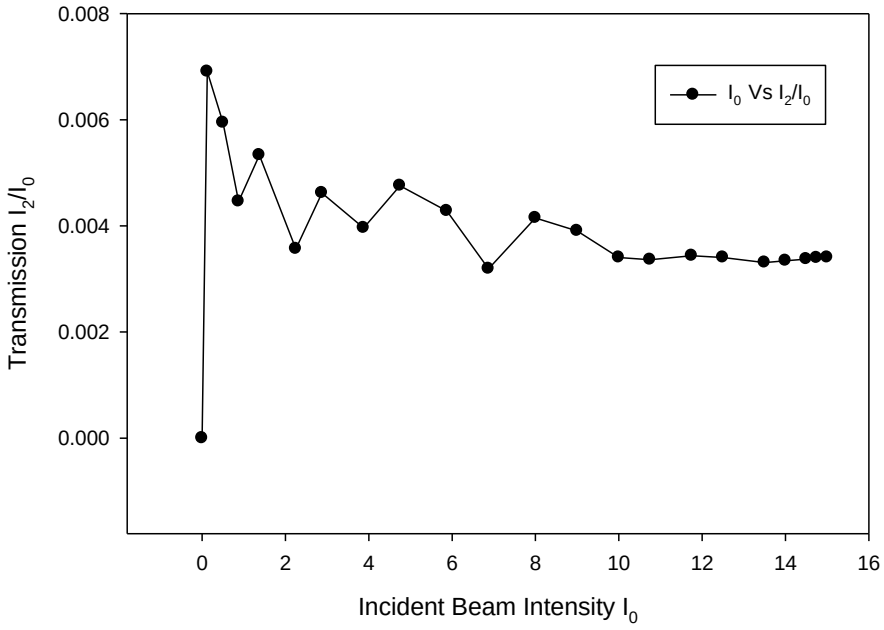

Figure 2.7. Transmission I_2 / I_0 vs incident beam intensity I_0

By analyzing all the three plots, a steady transmission of I_t / I_0, I_1 / I_0 and I_2 / I_0 from the range 10 to 15 of the incident beam intensity I_0 is observed. So, it is concluded that if the half-wave plate angle is fixed in between the angle range of 68° to 82°, more accurate data with less noise can be obtained.

2.3 Theory

In theoretical analysis, the following assumptions were made (Please see Fig. 2.4 for notations):

- The laser crystals are plane-parallel and, therefore, it is assumed that distance $AB = BC$
- The surface loss and reflectivity do not depend on the direction of propagation of the laser beam.
- Any absorption loss is negligibly small compared to the scattering loss.
- The laser crystal's surfaces are well polished and have no surface scattering loss.

Let the surface reflectivity be R_S. Then the reflectivity is found from the experimental measurements of the intensities of the incident beam I_0 and the first reflected beam I_1:

$$R_S = \frac{I_1}{I_0} \tag{2.1}$$

Let the surface transmission be T_S. Then the surface transmission is found from the measured surface reflectivity as:

$$T_S = 1 - R_S = 1 - \frac{I_1}{I_0} \tag{2.2}$$

Then the beam intensity transmitted by the first surface at point *A* can be calculated as:

$$I_A = I_0 T_S = I_0 \left(1 - \frac{I_1}{I_0}\right) \tag{2.3}$$

Let the volume transmission over distance *d* from point *A* to point *B* be T_v. Then the transmitted beam intensity at the point *B* is calculated as:

$$I_B = I_A T_v = I_0 \left(1 - \frac{I_1}{I_0}\right) T_v \tag{2.4}$$

After reflection from surface S_2 the beam intensity inside the crystal becomes:

$$I'_B = I_B R_S = I_0 \left(1 - \frac{I_1}{I_0}\right) T_v R_S = I_0 \left(1 - \frac{I_1}{I_0}\right) T_v \frac{I_1}{I_0} = I_1 \left(1 - \frac{I_1}{I_0}\right) T_v \tag{2.5}$$

This reflected beam will again propagate through the crystal to the point *C*. Since $AB = BC$, the volumetric transmission will again be equal to T_v. Therefore, the beam intensity at point *C* before reflection/transmission occurs is given by:

$$I_C = I'_B T_v = I_1 \left(1 - \frac{I_1}{I_0}\right) T_v^{\,2} \tag{2.6}$$

At point C the beam is transmitted by the surface. Therefore, its intensity (which is measured experimentally) can be calculated as:

$$I_2 = I_C T_S = I_1 \left(1 - \frac{I_1}{I_0}\right) T_v^{\,2} T_S = I_1 \left(1 - \frac{I_1}{I_0}\right)^2 T_v^{\,2}\ , \tag{2.7}$$

where expression (2.2) is used for T_s to obtain the final result.

From equation (2.7) now the total volumetric transmission can be derived by calculating from the measured intensities of the reflected beams:

$$T_v(refl) = \sqrt{\frac{I_2}{I_1}}\left(1-\frac{I_1}{I_0}\right)^{-1} \tag{2.8}$$

Alternatively, the volumetric transmission T_v can be obtained from our measurement of the transmitted beam intensity I_t. Recall that when the laser beam hits the second surface S_2, its intensity I_B before reflection/transmission occurs, is given by equation (2.4). Therefore, the intensity of the beam transmitted by the second surface can be calculated as:

$$I_t = I_B T_S = I_0\left(1-\frac{I_1}{I_0}\right)T_v T_S = I_0\left(1-\frac{I_1}{I_0}\right)^2 T_v \ , \tag{2.9}$$

where, expression (2.2) is used for T_s.

From equation (2.9) an alternate expression can be derived for calculation of the total volumetric transmission from measured intensity of the laser beam transmitted by the crystal:

$$T_v(trans) = \frac{I_t}{I_0}\left(1-\frac{I_1}{I_0}\right)^{-2} \tag{2.10}$$

It is noteworthy that if the experimental results are correct, it should be expected to obtain exactly the same estimates of the volumetric transmission T_v from both expressions (2.8) and (2.10) for all incident angles. Finally, using equations (2.8) and (2.10) we can obtain the effective absorption coefficient for the volumetric loss. In the first case of (2.8), the total distance that the light travels through the crystal is $AB + BC = 2d$, and therefore

$$k_a(refl) = \frac{1}{2d}\ln\left(\frac{1}{T_v(refl)}\right) \tag{2.11}$$

In the second case of the (2.10), the total distance traveled by the light through the volume is $AB = d$, and therefore the effective absorption coefficient is calculated as

$$k_a(trans) = \frac{1}{d}\ln\left(\frac{1}{T_v(trans)}\right) \tag{2.12}$$

At a given incident angle θ the distance d can be calculated (using simple geometrical considerations) as follows:

$$d(\theta) = \frac{D}{\sqrt{1-\left(\frac{\sin\theta}{n}\right)^2}}\ , \tag{2.13}$$

where *D*-is the physical thickness of the crystal, and *n*-is the refractive index of the crystal.

In conclusion, for reflected beams measurements, it is derived:

$$T_v(refl) = \sqrt{\frac{I_2(\theta)}{I_1(\theta)}}\left(1-\frac{I_1(\theta)}{I_0(\theta)}\right)^{-1} \tag{2.14}$$

$$k_a(refl) = \frac{1}{2d(\theta)}\ln\left(\frac{1}{T_v(refl)}\right)$$

For the transmitted beams measurements, it is derived:

$$T_v(trans) = \frac{I_t(\theta)}{I_0(\theta)}\left(1-\frac{I_1(\theta)}{I_0(\theta)}\right)^{-2} \tag{2.15}$$

$$k_a(trans) = \frac{1}{d(\theta)}\ln\left(\frac{1}{T_v(trans)}\right)$$

Although the incident beam intensity I_0 was constant for all measurements, it was actually monitored and recorded to account for noise and temporal fluctuations, thus it is written as a function of θ.

- Now the laser crystal surfaces assumed to have scattering losses (δ_S) in addition to reflection on each surface (R_s).

In this case equation (2.2) could be generalized as

$$T_S = 1 - R_S - \delta_S \tag{2.16}$$

Similar analysis as above gives us the following relations,

$$I_2^* = I_1 \left(1 - R_s - \delta_s\right)^2 T_v^2, \tag{2.17}$$

where, $R_S = I_1 / I_0$ as in equation (2.1). If I_2^* inserted into equation (2.8), we obtain,

$$T_v^{cal} = \sqrt{\frac{I_2^*}{I_1}} \left(1 - R_s\right)^{-1} = T_v \left(\frac{1 - R_s - \delta_s}{1 - R_s}\right) = T_v \left(1 - \frac{\delta_s}{1 - R}\right) \tag{2.18}$$

As one can see we will obtain calculated crystal transmission less than T_v. Making similar analysis for transmission measurements, we obtain

$$I_t^* = I_0 \left(1 - R_s - \delta_s\right)^2 T_v \tag{2.19}$$

In this case equation (2.10) could be written as

$$T_v^{calc} = \frac{I_t^*}{I_0} \left(1 - \frac{I_1}{I_0}\right)^{-2} = T_v \left(\frac{1 - R_s - \delta_s}{1 - R_s}\right)^2 = T_v \left(1 - \frac{\delta_s}{1 - R_s}\right)^2 \tag{2.20}$$

Taking in to account that $\delta_s / 1 - R_s < 1$ one can estimate that

$$T_v^{calc} \approx T_v \left(1 - \frac{2\delta_s}{1 - R_s}\right) \tag{2.21}$$

As we can see from equation (2.18) and (2.21), the calculated transmission ignoring surface losses are smaller than the real one. It means that our volume loss estimations provide us with the upper limit of this parameter. One can also see that the influence of

surface losses is higher on the accuracy of transmission measurements than on reflection measurements.

- Now the reflection from the output surface (R_{s2}) is assumed to differ from R_s and equals $R_{S2} = R_S + \delta R$, where δR could be positive or negative.

In this case we can rewrite

$$I_2^* = I_0(1-R_s)^2\left(R_s+\delta R\right)T_v^{\,2} = I_1(1-R_s)^2T_v^{\,2}\,\frac{\left(R_s+\delta R\right)}{R_s} \quad , \tag{2.22}$$

where, $R_S = I_1 / I_0$ as in equation (2.1). If I_2^* inserted into equation (2.8) then we will obtain:

$$T_v^{cal} = \sqrt{\frac{I_2^*}{I_1}}\left(1-R_s\right)^{-1} = T_v\sqrt{1+\frac{\delta R}{R_s}} \approx T_v\left(1+\frac{\delta R}{2R_s}\right) \tag{2.23}$$

Making similar analysis for transmission measurements, we will obtain

$$I_t^* = I_0\left(1-R_s-\delta R\right)(1-R_s)T_v \tag{2.24}$$

In this case equation (2.10) could be written as

$$T_v^{calc} = \frac{I_t^*}{I_0}\left(1-\frac{I_1}{I_0}\right)^{-2} = T_v\left(\frac{1-R_s-\delta R}{1-R_s}\right) = T_v\left(1-\frac{\delta R}{1-R_s}\right) \tag{2.25}$$

In this situation, if $2R_s < (1-R_s)$ or $R_s < 33\%$ the transmission measurements are less sensitive of δR. Also we can see the influence of δR has different sign for these two measurements.

CHAPTER 3

RESULTS AND DATA ANALYSIS

3.1 Validating the performance of experimental setup

The performance of experimental set-up has to be validated to make sure the correct data are obtained. This was done by measuring the surface reflection of the undoped ZnSe samples and comparing with the theoretical reflection calculated from the Fresnel's equation.

Measurements were conducted for two undoped ZnSe laser crystals with different lengths *D*, laser crystal with length $D = 0.840cm$ (hereafter will be referred as laser crystal 1) and laser crystal with length $D = 0.608cm$ (hereafter will be referred as laser crystal 2). Half-wave plate angle was set at 72°. Laser crystal was mounted on a mechanical rotator and by rotating the sample from incident angle 45° to 75° using mechanical rotational stage, beam intensities I_0, I_t, I_1 and I_2 were measured and recorded. Experimental reflection I_1 / I_0 was calculated. The theoretical reflection was calculated using the Fresnel's equation [13]:

$$R_{\exp} = \left[\frac{n_1 \sqrt{1 - \left(\frac{n_1}{n_2} \sin\theta \right)^2} - n_2 \cos\theta}{n_1 \sqrt{1 - \left(\frac{n_1}{n_2} \sin\theta \right)^2} + n_2 \cos\theta} \right]^2 \tag{3.1}$$

n_2 refers to the refractive index of the second medium which in our case is the undoped ZnSe laser crystal. n_2 was calculated using the Sellmeier equation[14]:

$$n_2 = \sqrt{9.01536 + \frac{0.24482}{\lambda^2 - (0.29934)^2} + \frac{7229.931303}{\lambda^2 - (48.38)^2}} = 2.59 \ , \tag{3.2}$$

where λ is the laser beam wavelength in μm and in our case it is $0.6328\,\mu m$.

n_1 refers to refractive index of the first medium, which was air. Substituting $n_1 = 1$ and $n_2 = 2.59$ into equation (3.1), the equation reduces to:

$$R_{\exp} = \left[\frac{\sqrt{1 - \left(\frac{\sin\theta}{2.59} \right)^2} - 2.59\cos\theta}{\sqrt{1 - \left(\frac{\sin\theta}{2.59} \right)^2} + 2.59\cos\theta} \right]^2 \tag{3.3}$$

Figures 3.1 and 3.2 show the plot for experimental and theoretical reflection I_1 / I_0 for incident angle 45-75° for laser crystal 1 and laser crystal 2, respectively. In both graphs, at lower angles the experimental reflection is seen to be in a good agreement with the theoretical reflection. However, as the incident angles get closer to the Brewster angle, which is the minimum of the curves, experimental reflection is higher than the theoretical reflection. In practice, due to scattering and absorption losses, the experimental reflection has to be lower than the theoretical reflection in both cases. The experimental reflection being higher than the theoretical reflection could be due to the

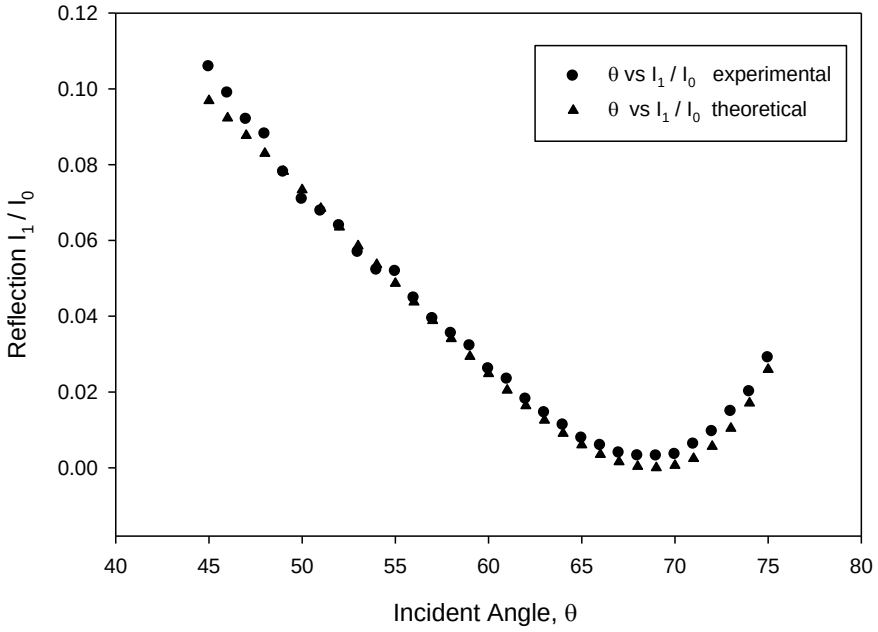

Figure 3.1. Experimental and theoretical reflection I_1 / I_0 for incident angle 45-75° of laser crystal 1.

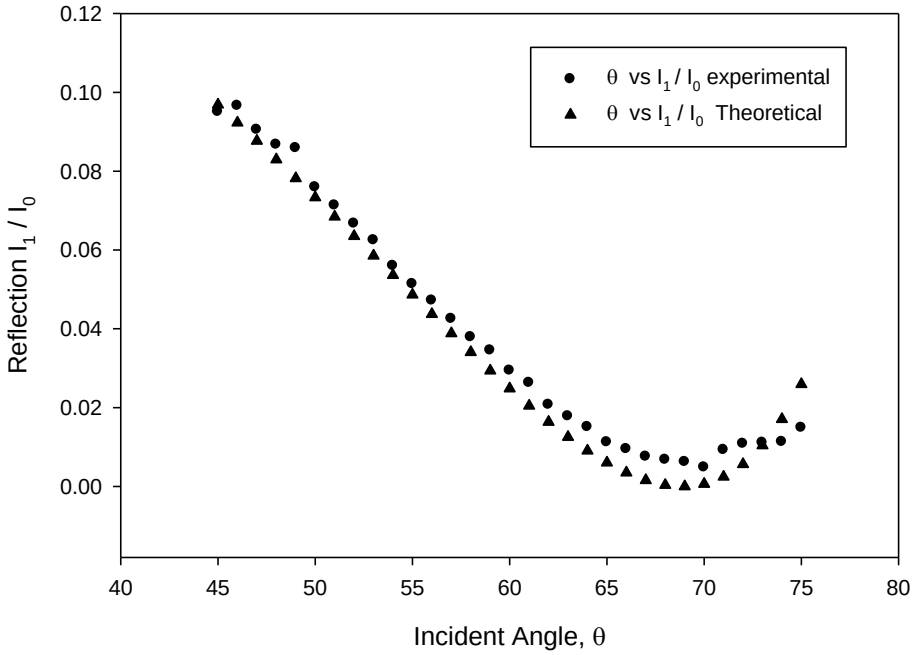

Figure 3.2. Experimental and theoretical reflection I_1 / I_0 for incident angle 45-75° of laser crystal 2.

surface scattered light that interferes the reflected beam, I_1 detection. Otherwise the experimental data show a good coincidence with the theoretical data. Both experimental and theoretical graphs follow the same curve, and the minimum of both graphs fall at the same point, which is known to be the Brewster angle. This validates the experimental data and demonstrates that they are reasonably good.

3.2 Extraction of effective absorption coefficient k_a

After confirming that the measured data from the developed method are valid, the total volumetric transmissions T_v and the effective absorption coefficients k_a for both laser crystals were calculated using equations (2.14) and (2.15). The dependence of these transmissions and absorption coefficients to the incident beam angle θ were graphed. As can be seen from Figures 3.1 and 3.2, ZnSe laser crystals has Brewster angle near 69° (the minimum). At this point, reflection approaches zero and measurements are sensitive to error such as k_a values approaching 0.. So the incident angles closer to Brewster angle have to be avoided. Since the experimental and theoretical reflections are in a good agreement at angles between 47.5 – 55.5°, the incident angle has been limited within 47.5 – 55.5° for loss estimation for both samples.

Figure 3.3 shows the dependence of the reflected and transmitted beams total volumetric transmission T_v to the incident beam angle θ for laser crystal 1. T_v (refl) refers to the total volumetric transmission calculated using the first surface reflected beam intensity, I_1, while T_v (trans) refers to the total volumetric transmission calculated using the second surface transmitted beam intensity, I_t. Figure 3.4 shows the dependence of the effective absorption coefficient k_a on the incident beam angle θ. k_a (refl) refers to the

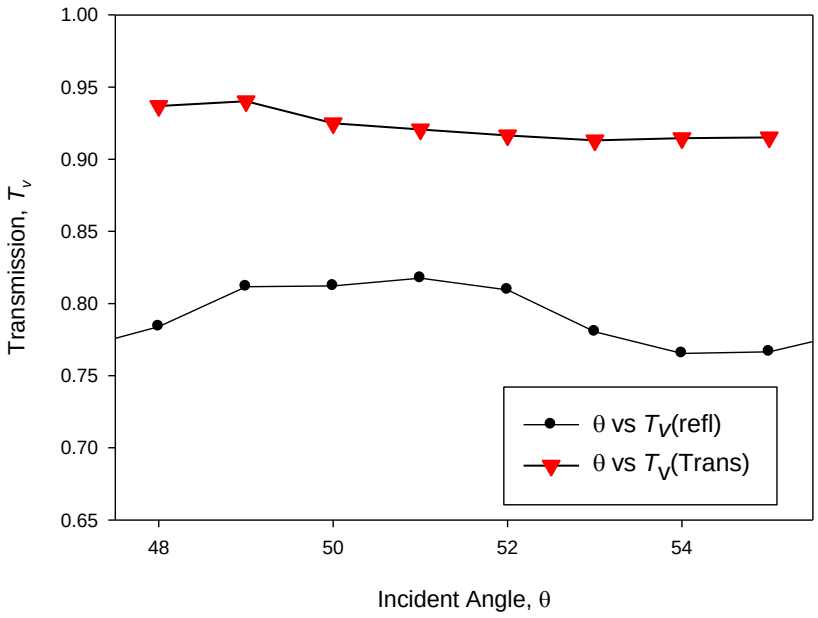

Figure 3.3. Laser crystal 1 reflected and transmitted beams transmission dependence vs incident beam angle θ.

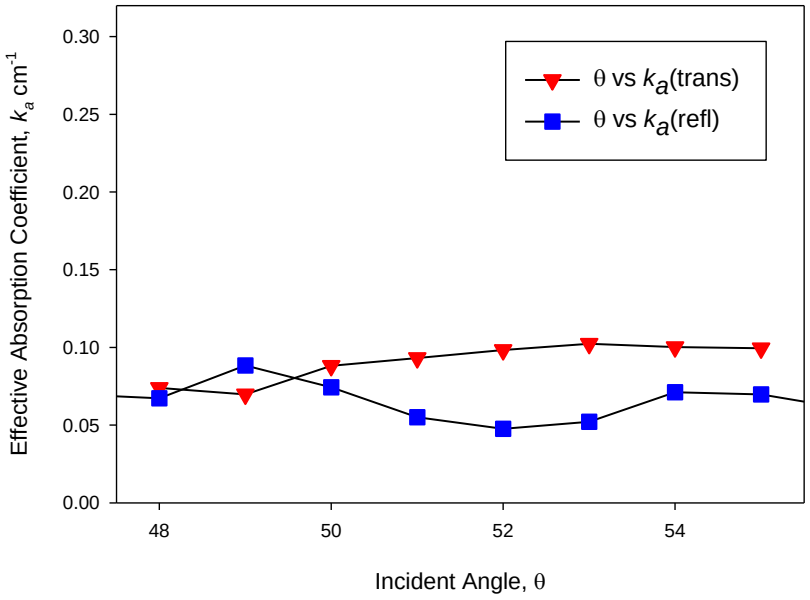

Figure 3.4. Laser crystal 1 reflected and transmitted beams effective absorption coefficient k_a dependence vs incident beam angle θ.

effective absorption coefficient calculated using T_v (refl), while k_a (trans) refers to the effective absorption coefficient calculated using T_v (trans).

Figure 3.5 shows the dependence of the reflected and transmitted beams total volumetric transmission T_v to the incident beam angle θ for laser crystal 2. Figure 3.6 shows the dependence of the effective absorption coefficient k_a to the incident beam angle θ.

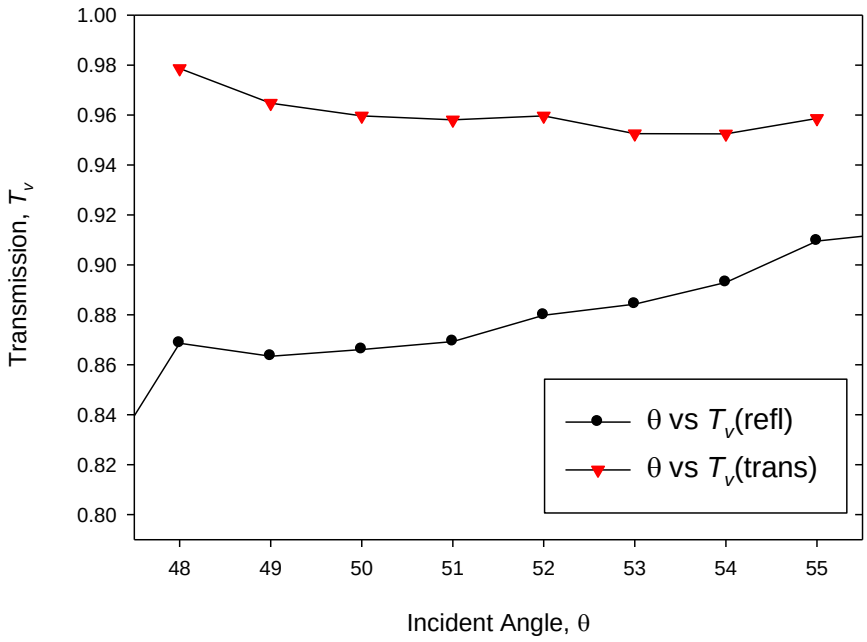

Figure 3.5. Laser crystal 2 reflected and transmitted beams transmission dependence vs incident beam angle θ.

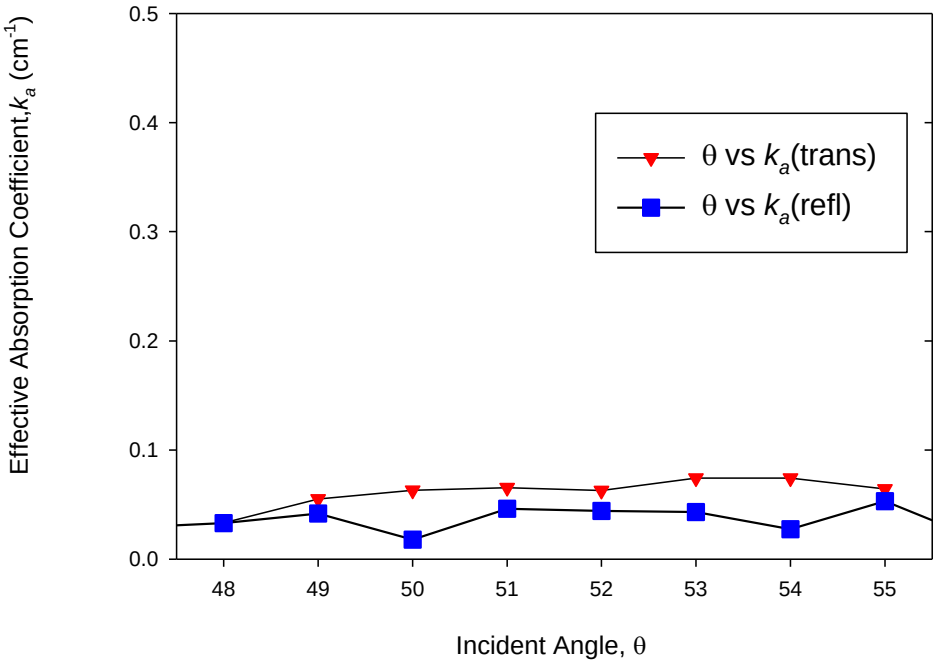

Figure 3.6. Laser crystal 2 reflected and transmitted beams effective absorption coefficient k_a dependence vs incident beam angle θ.

Ideally, the linear fits of the k_a *vs.* θ should be represented by coinciding horizontal lines whose y-axis intersection shows the measured average value of the effective loss coefficient k_a. However, due to measurement errors, scattered data with many different values of k_a were obtained. Therefore, in order to obtain more accurate value of k_a, the average of k_a was calculated.

The average k_a for laser crystal 1 calculated to be 0.078cm^{-1}, while for laser crystal 2 is 0.050cm^{-1}.

As known earlier, the obtained average k_a is the sum of internal absorption coefficient, k_{abs} and internal scattered coefficient, k_{scat}.

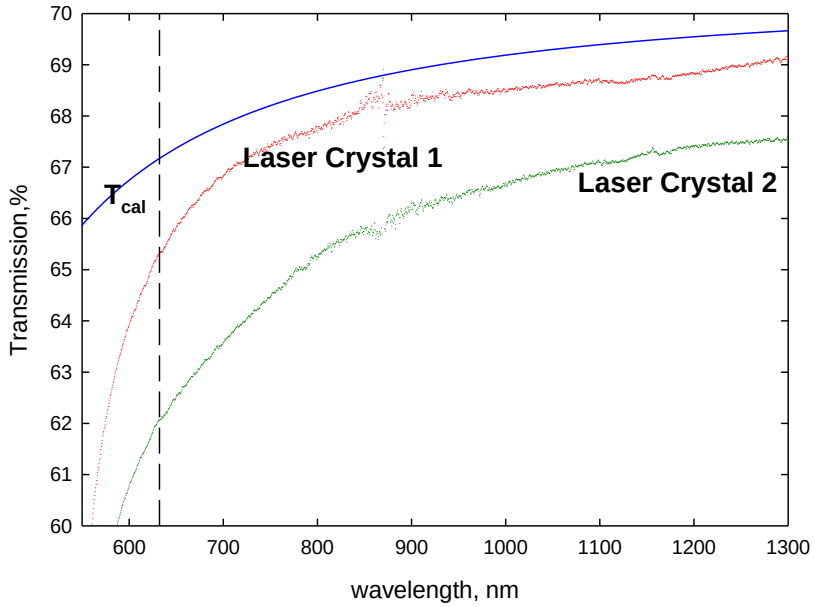

Figure 3.7. Internal Transmission Spectra of laser crystals 1 and 2.

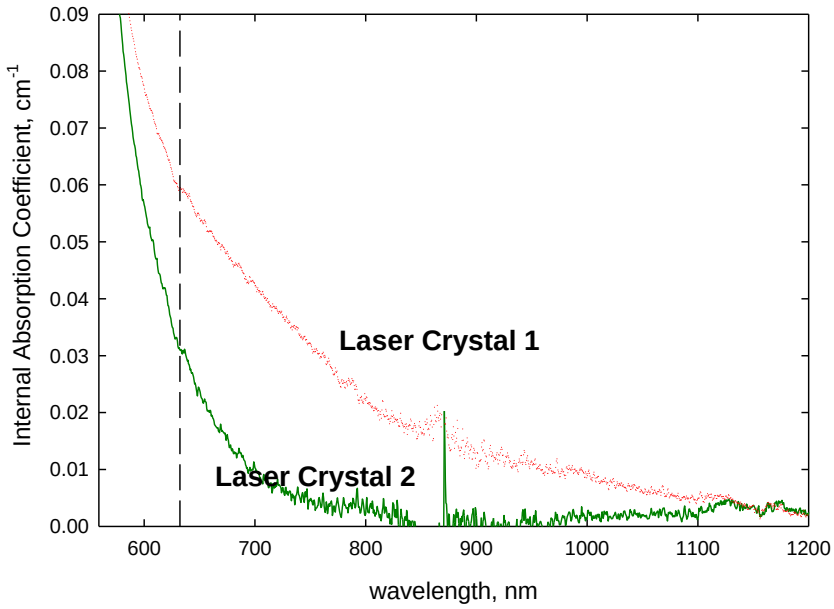

Figure 3.8. Wavelength dependence of internal absorption coefficient k_{abs}.

$$k_a = k_{abs} + k_{scat} \tag{3.4}$$

To discriminate between the internal absorption coefficient and the internal scattered coefficient, the internal absorption transmission of both laser crystals was measured with the spectrophotometer. Figure 3.7 shows the internal transmission spectra of both laser crystals measured over 500 – 3000nm spectral range. T_{cal} was plotted using equation,

$$T_{cal} = (1-R)^2 \sum_{m=0}^{\infty} R^{2m} = (1-R)^2 \sum_{m=0}^{1} R^{2m} = (1-R)^2 (1+R^2) \tag{3.5}$$

R was calculated for wavelengths λ using the Fresnel's equation (eq.3.1) where, the incident angle θ was substituted with *0*, and n_1 was substituted with *1* since it was the air medium. Then, Fresnel's equation reduced to,

$$R_{\exp}(\lambda) = \left(\frac{1-n_2(\lambda)}{1+n_2(\lambda)} \right)^2 \tag{3.6}$$

To extract the internal absorption coefficient, k_{abs} from this measurement, the k_{abs} wavelength dependence has been plotted by calculating the k_{abs} from equation,

$$T_{abs} = e^{-k_{abs}.D} = \frac{T_{abs}^{measured}}{T_{cal}}, \tag{3.5}$$

where D is the beam path length in the laser crystals. T_{abs} is normalized with respect to T_{cal} internal transmission obtained from Figure 3.7. Figure 3.8 shows the plot of k_{abs} wavelength dependence. At wavelength 632.8 nm, the internal absorption coefficients k_{abs} are $0.059cm^{-1}$ and $0.031cm^{-1}$ for laser crystal 1 and laser crystal 2, respectively.

Now, the internal scattered coefficient can be calculated by substituting the obtained above values into equation (3.4). For laser crystal 1, k_{scat} was $0.019cm^{-1}$, while for laser crystal 2, exactly the same value of $0.019cm^{-1}$ was obtained.

This analysis shows that both crystals have the same internal scattered coefficient this value is very close to the internal scattered coefficient measured by other techniques which was reported to be $0.020cm^{-1}$.

CHAPTER 4

CONCLUSION

In this investigation we developed a method for measurement of passive losses in Cr^{2+}:ZnSe and Cr^{2+}:ZnS laser crystals using polarized laser beam. Our method provides a basic practical knowledge on measuring the total losses in initial undoped polycrystalline ZnSe and extracting reflection, internal absorption and scattering losses from the total losses.

In this development, initially the transmission of polarized beam method was considered to separately measure scattering, reflection, and intrinsic losses in initial undoped polycrystalline ZnSe and ZnS host materials. During the experimental set-up it was noticed that the scattered beam intensity ratio to the transmitted and reflected beam intensity was extremely small. So, the front and back surface of the laser crystal scattered light intensity is considered negligible and decided not to be measured. The experimental set-up was reassembled and validated by measuring the front surface reflection transmission and its comparing with the theoretical data. Though the measured transmission was slightly higher than experimental, which was later understood that the surface scattered lights added to the reflection detection, the Brewster angle for both experimental and theoretical fall at the same angle and showed a good validation of the developed method.

Two undoped polycrystalline ZnSe samples with different lengths were used to measure the surface reflection. Effective absorption coefficient, k_a was extracted from these data, and the analysis showed that the longer ZnSe laser crystal has higher k_a

compared to the shorter one. The spectrophotometer measurement was conducted to extract the internal absorption coefficient, k_{abs}. Using the effective absorption coefficient and internal absorption coefficient the internal scattering coefficient was calculated. Similar value of $0.019cm^{-1}$ was obtained for both laser crystals.

We have demonstrated that the developed method is effective in measuring the passive losses in laser crystals. Future investigations will focus on using laser beam with wavelength 2500nm to avoid strong charge transfer absorption associated with $Cr^{2+} + e_v \rightarrow Cr^{+}$ transition in ZnS and ZnSe crystals, and to obtain more accurate measurement data. In future, Cr^{2+}:ZnSe and Cr^{2+}:ZnS will substitute the initially undoped ZnSe polycrystalline samples to identify major factors defining passive losses in Cr doped chalcogenides (Cr concentration, temperature and exposition time of annealing) for subsequent optimization of these parameters.

LIST OF REFERENCES

1. I. T. Sorokina, "*Cr^{2+}-doped II–VI materials for lasers and nonlinear optics*", Opt. Mater., vol.26, pp. 395–412 (2004).

2. H.Kukimoto, S. Shionoya, T. Koda, T. and R.Hioki, "*Infrared absorption due to donor states in ZnS crystals*, " J. Phys. Chem. Solids, 29, 935-940 (1968).

3. C-H.Su, S. Feth, M.P. Voltz, R. Matyi, M.A. George, K. Chattopadhyay, A. Burger, S.L.Lehoczky, "*Vapor growth and characterization of Cr-doped ZnSe crystals*, " J. Crystal Growth 207, 35-42 (1999).

4. D.R.Vij, N. Singh, "*Luminescence and related properties of II-VI semiconductors*, " (Nova Science Publishers, Inc, Commack, NY, 1998).

5. J.-O.Ndap, K. Chattopadhyay, O.O. Adetunji, D.E. Zelmon, A. Burger, "*Thermal diffusion of Cr^{2+} in bulk ZnSe*, " J. of Crystal Growth, 240,176-184 (2002).

6. K. C. Kao and T. W. Davies, "*Spectrophotometric studies of ultra low loss optical glasses I: single beam method*, " J. Sci. Instrum. 2;1, 1063 (1968)

7. M. W. Jones and K. C. Kao, "*Spectrophotometric studies of ultra low loss optical glasses II: double beam method*," J. Sci. Instrum. 2;2, 331 (1969).

8. D. A. Pinnow and T. C. Rich, "*Development of a Calorimetric Method for Making Precision Optical Absorption Measurements*," Appl. Opt. 12, 984 (1973).

9. H.-H. Witte, "*Determination of Low Bulk Absorption Coefficients*," Appl. Opt. 11, 777 (1972).

10. A. R. Tynes, Bell Lab. Rec. 50, 302 (1972).

11. A. R. Tynes, A. D. Pearson, and D. L. Bisbee, "*Loss Mechanisms and Measurements in Clad Glass Fibers and Bulk Glass*," J. Opt. Soc. Am.61, 143 (1971).

12. D. B. Keck and R. Tynes, "*Spectral Response of Low-Loss Optical Waveguides*," Appl. Opt. 11, 1502-1506 (1972)

13. Hecht, Eugene, *Optics*, 2nd ed. (1987), pg.100.

14. David N.Nikogosyan, *Properties of Optical and Laser-Related Materials*, pg.291.